Molecular dynamics simulation of local structure of aluminium and copper in supercooled liquid and solid state by using EAM

1995 J. Phys.: Condens. Matter 7 2379

(http://iopscience.iop.org/0953-8984/7/12/003)

J. Phys.: Condens. Matter 7 (1995) 2379–2394. Printed in the UK

Molecular dynamics simulation of local structure of aluminium and copper in supercooled liquid and solid state by using EAM

Chen Kuiying†, Liu Hongbo†, Li Xiaoping‡, Han Qiyong‡ and Hu Zhuangqi†

† State Key Laboratory of RSA, Institute of Metal Research, Academia Sinica, Shenyang 110015, People's Republic of China

‡ Department of Physical Chemistry of Metallurgy, University of Science and Technology Beijing, Beijing 100083, People's Republic of China

Received 30 November 1994, in final form 1 February 1995

Abstract. Based on the embedded-atom method, molecular dynamics simulations have been performed to study the structural features of Al and Cu in the liquid and solid states during rapid solidification. The calculated pair correlation functions above the melting points of Al and Cu are found to be in good agreement with experiment, especially for Cu. The results show that the EAM can correctly and efficiently predict the glass transition and crystallization during rapid solidification from liquid metals, and can also describe microstructures of liquids, supercooled liquids, glasses and crystalline phases. In addition, structural analysis using bond orientational order and pair analysis techniques have been made in detail, and the effect of cooling rate on microstructures during rapid solidification has been analysed.

1. Introduction

Recent years have witnessed considerable progress in the development of empirical or semi-empirical many-body potentials for accurately reproducing thermodynamic and structural properties of most transition metals. One feature of these many-body potentials is easy to carry out for computer simulations. The embedded-atom method (EAM) of Daw and Baskes [1, 2] (and further developed by Johnson *et al* [3–6]), N-body potentials proposed by Finnis and Sinclair (FS) [7] (and further developed by Ackland *et al* [8–10]) and the tight-binding model of many-body potentials given by Rosato *et al* [11] consist of three main aspects of the present empirical or semi-empirical many-body potentials.

The EAM based on the density functional [12] and quasi-atom concept [13] has been successfully applied to a wide range of aspects in the solid state, such as in point defects, dislocations and surfaces [14–16]. Foiles [17] used an earlier set of EAM functions to calculate properties of bulk liquids, and got reasonable results compared with experiment. Mei *et al* [18] applied the nearest-neighbour model of EAM proposed by Johnson [3] to the liquid state by using molecular dynamics simulations; the results for structure factors and diffusive coefficients of noble metals are in good agreement with experiments. Furthermore, Mei extended the nearest-neighbour model of EAM to the third-neighbour situation [19]. Based on his extended model, Mei evaluated thermodynamic properties for noble metals, and the free energy for aluminium [20]. It should be noted that the liquid state is qualitatively different from the other applications of the EAM method and so will provide a critical test of the range of applicability of the methods as well as the empirical procedures used to derive

0953-8984/95/122379+16$19.50

the EAM functions. It is known to us that in the determination of embedding functions and pair potentials, only information about small deviations from the equilibrium solid are used. Therefore, it is not clear as to whether these functions will reasonably describe systems such as liquids, especially supercooled liquids and glasses. Thus liquid-state calculations (especially supercooled liquids) would provide a test of the form of the embedding functions at lower than usual electron densities. As pointed out by Foiles [17], the motion of the atoms in liquid brings them much closer together at times than is found in the equilibrium solid. Conversely, the liquid data can be used to improve the choice of the functional forms. One way to enhance the reliability of the EAM for calculating the properties of liquids may be to fit the EAM functions to properties of bulk liquids. Doing so would allow the EAM to accurately predict the behaviour of liquids for a wider range of characterizations. In addition, the application of the EAM to a supercooled liquid shows promise for finding theoretical values of properties that cannot be determined experimentally.

The FS type of potential based on the second-moment approximation of the tight-binding theory is another type of many-body potential, which is constructed to deal with BCC-like structures. Ackland [8] extended the FS type of potential by adding the potentials' cores, fitted to electron gas calculations. The adjusted potentials are shown to predict a more realistic pressure–volume relationship. Holender [21,22] applied the FS type of many-body potential to the liquid state for pure noble metals, such as for Ag, Au and Cu. The structure factors and thermodynamic properties thus obtained by using MDS are in good agreement with experiment. Kulp *et al* [23,24] used Ackland's model for binary Cu–Ti alloys with the help of MDS. Their results demonstrate that FS-type potentials can give reasonable results when compared with experiment. The tight-binding model many-body potentials proposed by Roasto *et al* are another important type of potential, and have been successfully used to investigate amorphization of Ni–Zr alloy and quenching from the liquid state [25,26]. Holzman *et al* [27], in research on properties of bulk liquid and surface energy, argued that the further application of EAM should be on liquids' supercooled liquid aspects. Unfortunately, up till now, a study of this aspect has not been made. Here, we chose the EAM as the fundamental model, though these EAM functions are parametrized to bulk solid properties. We want to see if the EAM can correctly and efficiently describe the glass transition and crystallization during rapid cooling from the liquid state. These problems comprise the main subject of the research. In the present paper, we chose aluminium (FCC structure, sp-bonded metal) and copper (FCC structure, transition metal) as candidates. We used the pair correlation function, the bond orientational order and pair analysis techniques as geometrical functions to examine the features of structure for both Al and Cu in liquid and solid state.

2. Theory procedure

In the frame of EAM [2], the total energy of an N-atom system takes the form

$$E_{\text{tot}} = \sum_i F_i(\rho_i) + \frac{1}{2}\sum_{\substack{i,j \\ i \neq j}} \Phi_{ij}(r_{ij}) \tag{1}$$

where ρ_i is the electronic density at site i due to the surrounding atoms, $F_i(\rho_i)$ is the energy needed to embed an atom into this density, and $\Phi_{ij}(r_{ij})$ is the two-body central potential.

For aluminium and copper metals, the spherical approximation for the electronic density is made and electronic density is approximated by the superposition of atomic densities

$$\rho_i = \sum_{j \neq i} f_j(r_{ij}) \tag{2}$$

where $f_j(r_{ij})$ is the contribution to the electronic density at atom i due to atom j at a distance r_{ij} from atom i. By replacing the atomic electronic density with an exponentially decaying function, Johnson [3] developed a set of simplified EAM functions for FCC metals. These analytic EAM functions are valid for nearest-neighbour interactions that are easy to use for computer simulations. Mei [19] obtained a simple analytic form of EAM-type potentials for dynamic simulation by extending Johnson's nearest-neighbour model to make it valid for any choice of cut-off distance. We chose Mei's model as the practical and fundamental model; the electronic density $f(r)$ is chosen as

$$f(r) = f_e \sum_{l=0}^{6} c_l (r_e/r)^l. \tag{3}$$

The two-body potential $\Phi(r)$ is

$$\Phi(r) = -\phi_e\Big(1 + \delta(r/r_e - 1)\Big) \exp\big(-\gamma(r/r_e - 1)\big). \tag{4}$$

Thus based on Rose's relation [28], the embedded energy in Mei's model can be written as

$$F(\rho) = E_c\left(1 - \frac{\alpha}{\beta}\ln\left(\frac{\rho}{\rho_e}\right)\right)\left(\frac{\rho}{\rho_e}\right)^{\alpha/\beta} + \frac{1}{2}\phi_e \sum S_m \exp\big(-(p_m - 1)\gamma\big)$$
$$\times \left(1 + (p_m - 1)\delta - p_m \frac{\delta}{\beta}\ln\left(\frac{\rho}{\rho_e}\right)\right)\left(\frac{\rho}{\rho_e}\right)^{p_m\gamma/\beta}. \tag{5}$$

Model parameters appearing in expressions (1)–(5) have been described in detail in [19], and the cut-off function used for simulation from Mei is

$$c(r) = \begin{cases} 1 & r \leqslant r_n \\ (1-x)^3(1 + 3x + 6x^2) & r_n < r < r_c \\ 0 & r > r_c \end{cases} \tag{6}$$

where $x = (r - r_n)/(r_c - r_n)$, $r_n = 1.75r_e$, $r_c = 1.95r_e$. Expressions (1)–(5) consist of the fundamental of our present calculations.

3. Molecular dynamic simulation approach

The molecular dynamic simulations are performed in a cubic box subject to periodical boundary conditions for a system with 500 particles. The time unit is chosen as 0.412×10^{-14} s and the time step is 5.0×10^{-15} s. Here, we chose the damped force method to decrease the temperature by forcing the bath temperature to change linearly at every step. In our study, we have performed the following type of calculation on aluminium and copper.

(i) In order to get an equilibrium liquid state, we start at 1323 K, 1023 K for Al and 1600 K for Cu respectively, which are higher than the melting points by 390 K, 90 K and 244 K. The systems are run for 3.0×10^5 time steps at these three temperatures.

(ii) Fast cooling from the liquid at 1323 K and 1600 K for aluminium and copper to the glass state at 100 K with a fast cooling rate 4.2×10^{13} K s^{-1}, with the aim to arrive at a glass state, and also examine the structural features of supercooled liquids of Al and Cu.

(iii) Slow cooling from the supercooled liquid state at 800 K for Cu to the crystal state at 100 K with a cooling rate 3.8×10^{11} K s^{-1}, to examine the processing of crystallization and also the structure.

During each quenching, the structural configurations were recorded at every fixed temperature interval. Then the structure analysis of liquid, supercooled liquid, glass and crystal was performed by RDF, bond orientational order and pair analysis techniques. The RDFs were obtained for 6×10^3 time steps, and results by bond orientational order and pair analysis techniques are averaged over 20 configurations. The whole calculations were carried out on a DEC 5000/125 workstation in our laboratory.

4. Structural description

4.1. Pair correlation function

The pair correlation function (PCF) has been widely used to describe the structure characterization of liquid and amorphous states; it is usually defined as [29]

$$\rho g(r) = N^{-1}\left\langle \sum_{i \neq j} \delta\big(r + R_i - R_j\big) \right\rangle \tag{7}$$

which $g(r)$ is the probability of finding an atom in the range from r to $r + \mathrm{d}r$, ρ is the average density of the system. R is the atoms' position, the angular bracket denotes the time average, and δ is the Dirac delta function.

4.2. Bond orientational order

In order to analyse the liquid structural characteristics, we shall measure local orientational symmetry in liquid metals with bond orientational order parameters. The importance of local orientational symmetries in three dimensions was emphasized over forty years ago by Frank [30]. Three-dimensional bond orientational order has been studied theoretically by Nelson and Toner [31]. Since then Steinhardt *et al* [32,33] have applied it in the simulation of supercooled Lennard-Jones liquids and in the examination of possible local and extended icosahedral bond order. For realistic metals or alloys, much less work has been devoted to their three-dimensional order. Thus, in our present research we shall measure local orientational symmetries in the computer generated models of liquids and solids. However, our attention is restricted to various icosahedral symmetries, Frank–Kasper (FK) polyhedra and Bernal hole polyhedra defined by bond orientational order and the pair analysis approaches (discussed below) respectively.

In liquid metals, any two atoms form a bond if they are within a separation chosen to equal the first minimal position of the RDF. The bond is described in terms of orientational order parameters Q_{lm}

$$Q_{lm}(r) = Y(\theta(r), \phi(r)) \qquad m = -l, \ldots, 0, \ldots, l \tag{8}$$

where $Y_{lm}(\theta(r), \varphi(r))$ are spherical harmonics; θ and φ are the polar angles of the bond measured with respect to some coordinate system.

In the case of clusters of particular interest, the averaged orientational order parameter should be considered

$$\overline{Q}_{lm}(r) = \langle Q_{lm}(r) \rangle \tag{9}$$

where the average is taken over all bonds within the cluster. In order to eliminate the dependence of Q_{lm} on a special coordinate system, it is important to consider the rotational invariant combination

$$Q_l = \left(\frac{4\pi}{2l+1} \sum_{m=-1}^{l} |\overline{Q}_{lm}|^2 \right)^{1/2}. \tag{10}$$

It is clear to see that Q_l is a quadratic invariant of Q_{lm}. For an icosahedral symmetry, it is sufficient to calculate the orientational order parameter W_6, which is most sensible with respect to the icosahedral symmetry suggested by Steinhardt [33]. W_6, being the third-order invariant of Q_{lm}, is defined as

$$\hat{W}_6 = \frac{W_6}{[\sum_{m=-6}^{6} |\overline{Q}_{6m}|^2]^{3/2}} \tag{11}$$

in which $W_6 = \sum_{m_1+m_2+m_3=0}^{m_1,m_2,m_3} \begin{bmatrix} 6 & 6 & 6 \\ m_1 & m_2 & m_3 \end{bmatrix} Q_{6m_1} Q_{6m_2} Q_{6m_3}$. This quantity is normalized so that it is independent of the overall magnitude of $\{Q_{lm}\}$. The order parameters Q_6 and W_6 measure the icosahedral ordering to some extent as argued by Steinhardt [33], and for an ideal icosahedron, the absolute value of W_6 gives the maximum number 0.169 754 [33].

4.3. Pair analysis techniques

In the present paper, structural analysis by the PA method [34] is also used in the calculation. If two atoms are within a given cut-off separation, here chosen to equal the position of the first minimum in the appropriate PDF, we say that these two atoms form a bond. Based on the PA formula, the fivefold symmetry bond plus other different kinds of bond can be obtained by computer. The *1551* bonded pairs represent the two root pair atoms with five common neighbours that have five bonds which form a pentagon of near-neighbour contact. Similar analysis holds for 1441, 1661 bonded pairs, etc. It is necessary to point out that the number of 1551 bonded pairs in a liquid is a direct measurement of the degree of icosahedral ordering. By using the PA formula, we can count several polyhedra with various symmetries. If only the centre atom has twelve neighbouring atoms, and they are all joined to the centre atom by twelve 1551 bonded pairs, we say they form an icosahedron. Similarly, if the centre atom has fourteen (or more) neighbouring atoms, twelve of which are joined to the centre atom by twelve 1551 bonded pairs and two (or more) of which are joined to the centre atom by two 1661 bonded pairs, then they define a FK polyhedron with the coordinate number $Z = 14$. For other FK polyhedra with different coordinate numbers, the definition still holds. In the same way, we can define a Bernal hole polyhedron [35]. In addition, a polyhedron consisting of only 1551, 1441 and 1661 bonded pairs is called a defective icosahedron.

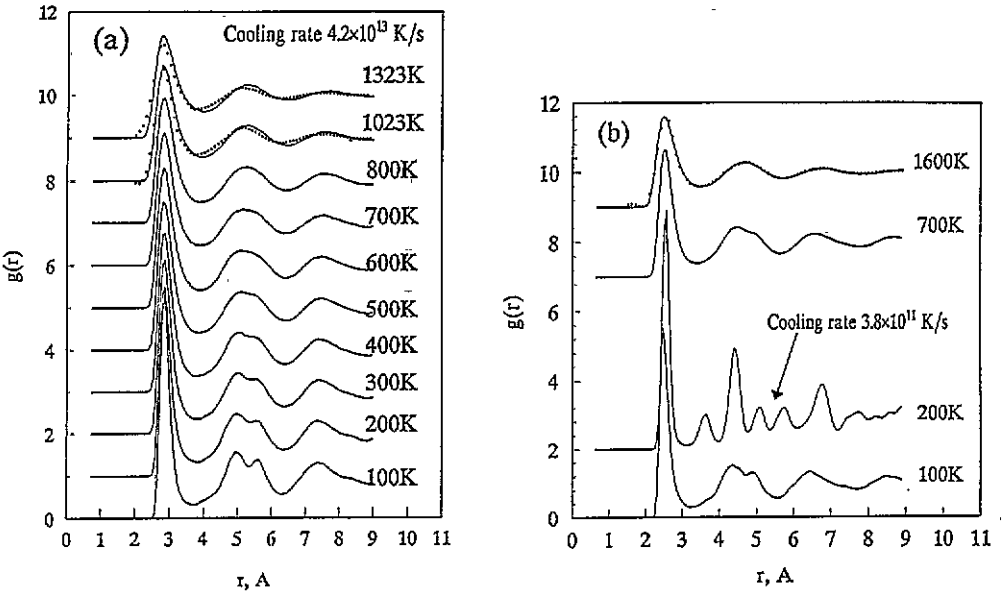

Figure 1. Pair correlation functions for Al (*a*) and Cu (*b*) in the liquid, supercooled liquid and solid states. Solid lines are calculated results, whereas dotted lines are from experiments [42].

5. Results and discussion

5.1. Fast-cooling processing and glass formation

In the following section, we first study the fast-cooling process of liquid Al and Cu metals, and examine the structural features in the liquid, supercooled liquid, amorphous state and crystal by several geometrical functions. Two curves in figure 1(*a*) which are at 1323 K and 1023 K for Al and a curve in figure 1(*b*) which is at 1600 K for Cu show that PCFs thus calculated based on expression (7) are very close to experiment [42], especially for copper, indicating the structures simulated at 1323 K, 1023 K and 1600 K are at the equilibrium liquid state respectively. It also demonstrates that the EAM functions are capable of providing a good description of the liquid state. Thus we obtain good starting points for the next series of rapid-cooling processing. In addition, figure 1 gives the PCFs for Al and Cu in the supercooled liquid and solid states during fast cooling, and corresponding temperatures at each state have been labelled for each curve respectively. We observe from figure 1 that during fast-cooling processing, the splitting of the second peak in PCFs gradually appears, and at the final temperature (100 K) for both Al and Cu in the present simulation, the second peaks have been split completely into two subpeaks which are known to us as a feature of the glass state. Furthermore, from figure 1 PCFs, we can determine the glass transition temperature at the present cooling rate 4.2×10^{13} K s^{-1} by an approach proposed by Abraham [36]. Figure 2 gives the relationship between g_{min}/g_{max} and temperature as suggested by Abraham, where g_{min} and g_{max} stand for the first minima and the maximum values of the corresponding PCF respectively. There exist two lines with different slopes in figure 2, and their intersections are the glass transition temperatures T_g, which are 420 K and 710 K for Al and Cu respectively. Based on T_g, we find that the second peak splitting has already appeared even in the supercooled liquid state, which is consistent with results

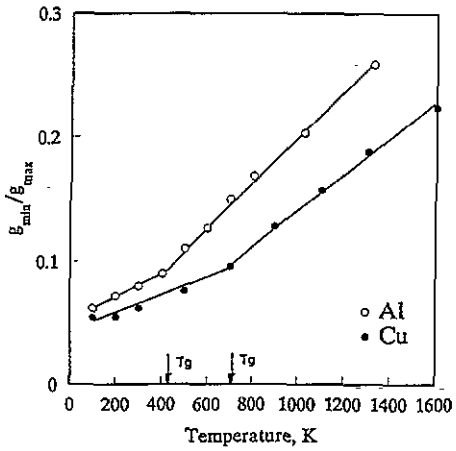

Figure 2. The relationship between g_{min}/g_{max} and temperature for Al and Cu during rapid solidification.

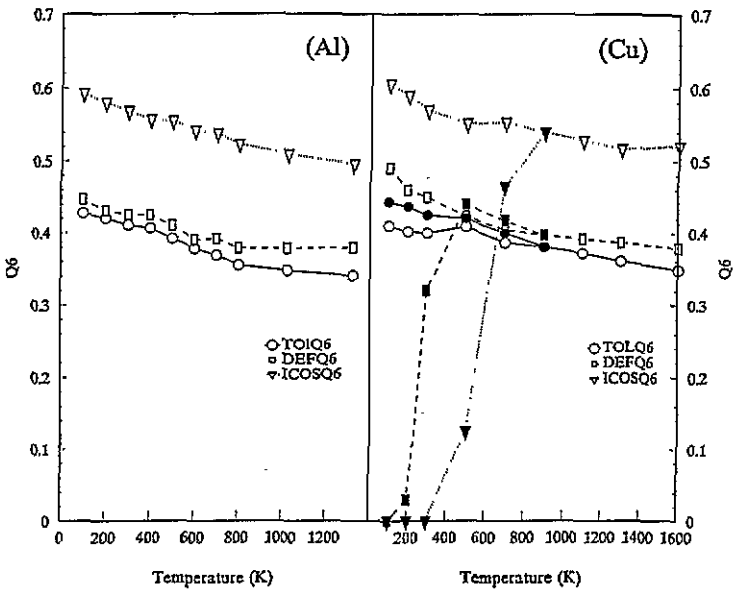

Figure 3. Bond orientational order parameters Q_6 for Al in (*a*) and Cu in (*b*) upon cooling. Open symbols in (*a*) and (*b*) represent Q_6 at cooling rate 4.2×10^{13} K s^{-1}, whereas the solid symbols in (*b*) represent results at the cooling rate 3.8×10^{11} K s^{-1}.

in [37, 38]. Thus the EAM-type potentials can indeed describe the glass transition processing and microstructures of supercooled liquid and amorphous solid.

In order to examine the fine structural features, apart from the PCFs, we will adopt bond orientational order parameters Q_6 and W_6 as geometrical functions. This can effectively describe the local symmetries of atom arrangement; the formula of this method has been described in detail in section 4. In our present research, we have calculated three kinds of

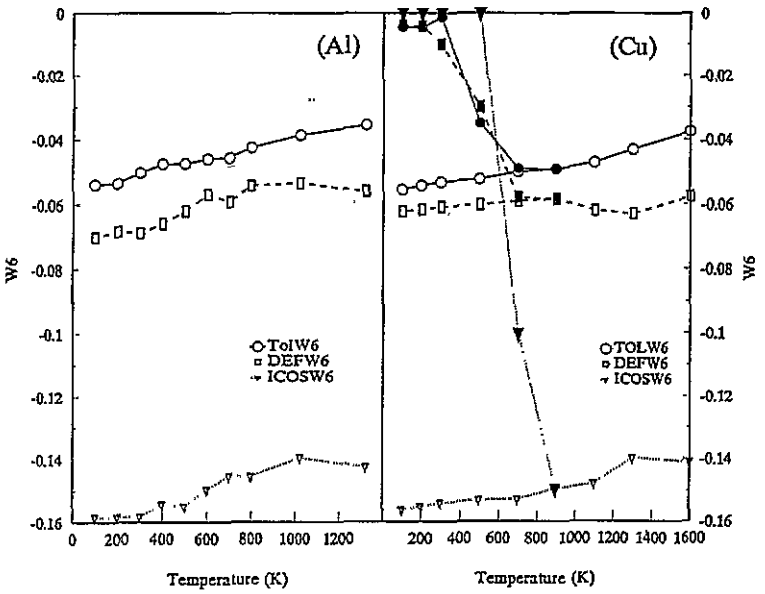

Figure 4. Bond orientational order parameters W_6 for Al in (*a*) and Cu in (*b*) upon cooling. Open symbols in (*a*) and (*b*) represent W_6 at cooling rate 4.2×10^{13} K s^{-1}, solid symbols in (*b*) present W_6 at the cooling rate 3.8×10^{11} K s^{-1}.

bond orientational order parameter. The icosahedral bond orientational order Q_6 (hereafter shortened to ICOSQ_6) has been calculated for the icosahedral cluster, and finally we chose an average value. The defective icosahedral bond orientational order parameter Q_6 (hereafter designated as DEFQ_6) has been calculated for the defective icosahedral cluster which has been defined in section 4.3. Finally, the total bond orientational bond parameter Q_6 (hereafter abbreviated to TOLQ_6) has been calculated for all clusters without distinguishing whether they are icosahedra, defective icosahedra or not. For the detailed meaning, readers are referred to our previous paper [40]. It is observed from figure 3 that with decreasing temperature (such as in the supercooled liquid region as well as the glass state), ICOSQ_6 for both Al and Cu gradually increases, indicating the icosahedral ordering has been enhanced. In addition, from the characterizations of DEFQ_6 and TOLQ_6, it is further found that the average icosahedral ordering has also become significant to some extent, and we will discuss this problem by the third-rotational invariant of W_6 below. The distribution of W_6 in figure 4 allows us to arrive at a conclusion that this gives a similar physical result for icosahedral ordering as presented in figure 3. Figure 4 further points out that with decreasing temperature, the perfection of icosahedra increases, nearly reaching the ideal icosahedra at 100 K from the behaviour of W_6.

Figure 5 presents the relative number of 1551 and 1541 bonded pairs of Al and Cu versus temperature. Figure 5 indicates that during fast cooling, the number of both 1551 and 1541 bonded pairs increases. Around T_g, the number of both 1551 and 1541 bonded pairs still increases, but no sharp increase of these two bonded pairs is observed. This result primarily clarifies that the structure of glasses may have a resemblance to the structure of the corresponding supercooled liquid, and we will further examine this point from other kinds of bonded pair. Figure 6 shows the relationship between the number of 1421 and 1422 bonded

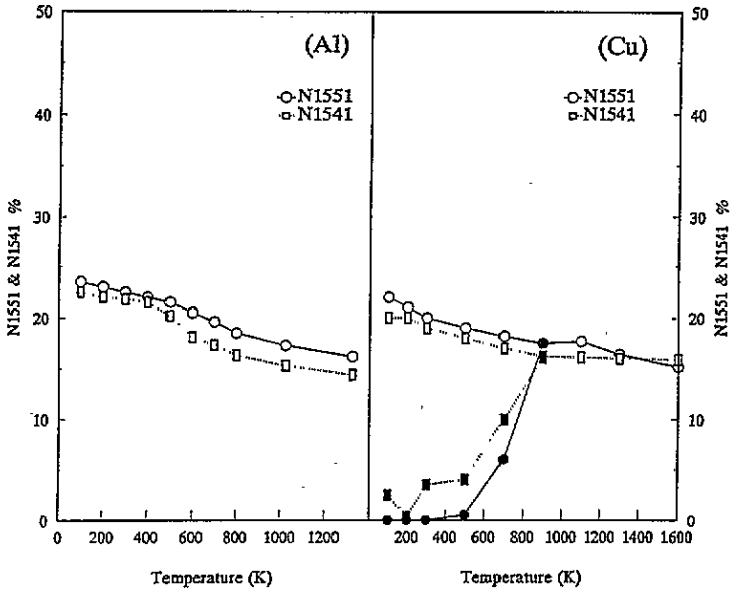

Figure 5. The relationship between the number of 1551 and 1541 bonded pairs and temperature during rapid solidification whose cooling conditions are the same as in figure 4.

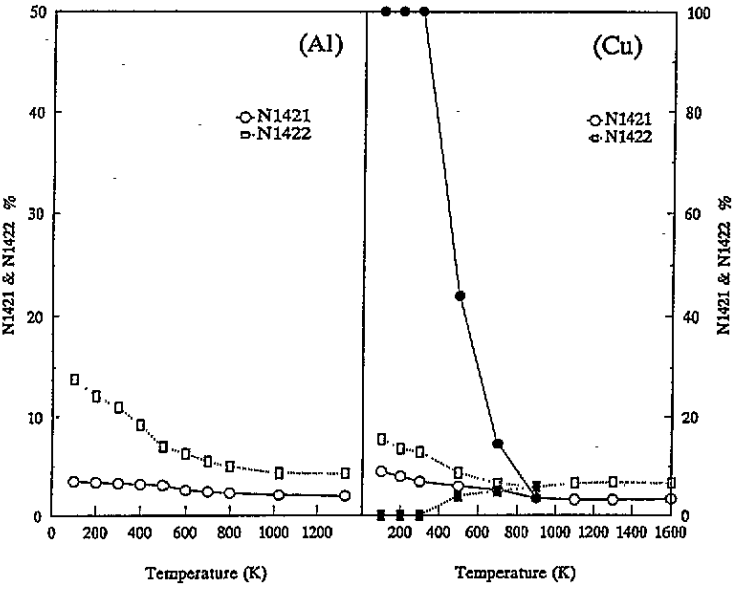

Figure 6. The relationship between the number of 1421 and 1422 bonded pairs and temperature during rapid solidification whose cooling conditions are the same as in figure 4.

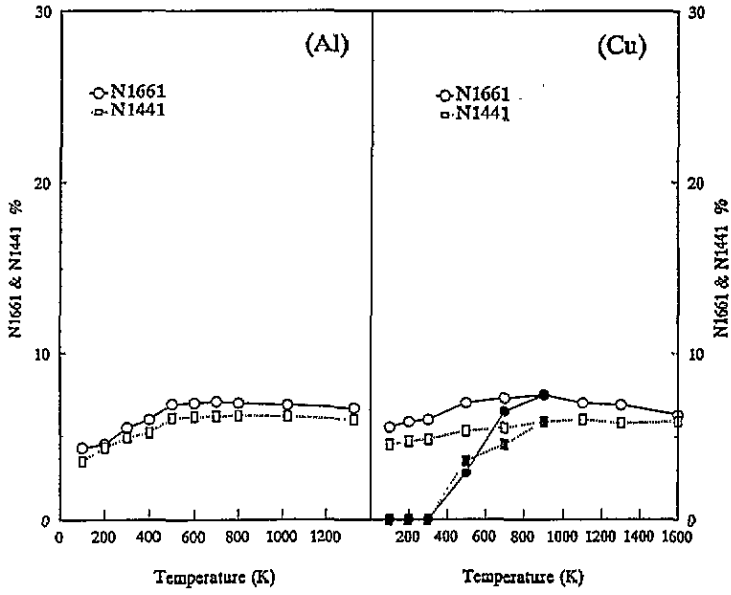

Figure 7. The relationship between the number of 1661 and 1441 bonded pairs and temperature during rapid solidification whose cooling conditions are the same as in figure 4.

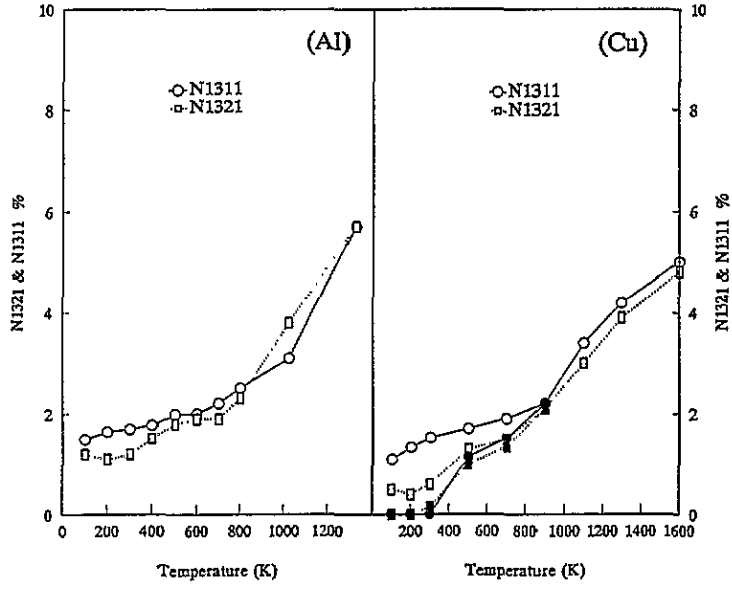

Figure 8. The relationship between the number of 1321 and 1311 bonded pairs and temperature during rapid solidification whose cooling conditions are the same as in figure 4.

pairs and temperature. It is found that the number of 1422 bonded pairs increases with decreasing temperature, whereas the number of 1421 bonded pairs changes only slightly in the whole temperature range studied here at the cooling rate 4.2×10^{13} K s^{-1}. It is known to us that the 1421 and 1422 bonded pairs represent the FCC-like and HCP-like structure [39] respectively. Hence, results in figure 6 demonstrate that dynamics (such as the fast cooling rate in the present paper) may produce an increase of 1422 bonded pairs (HCP-like structure) rather than the 1421 bonded pairs (FCC-like structure). That is to say the fast cooling of liquid favours the HCP-like structure if compared with the FCC-like structure from the point of view of the PA formula in some sense. This results leads to the conclusion that evolution of microstructure may take place under the control of dynamics. This conclusion will be further tested in the following section by using other kinds of bonded pair. Figure 7 gives the relative number of 1661 and 1441 bonded pairs versus temperature. We find that both these bonded pairs follow the same trends versus temperature, and with further decreasing temperature, both bonded pairs decrease at a slower rate. In addition, it is known to us that both the 1441 and 1661 bonded pairs behave like a BCC-type structure [39]. Thus, from the characterization of 1441 and 1661 bonded pairs, we note that the fast cooling (dynamics) does not favour BCC-type structure in Al and Cu metals. That is to say, in the competition processing controlled by dynamics, both 1441 and 1661 bonded pairs are gradually discarded. This results supports the point obtained in figure 6. Figure 8 shows the relative number of 1321 and 1311 bonded pairs versus temperature. Though the total number of these bonded pairs is very small if compared with other kinds of bonded pair, its evolution behaviour during rapid solidification may provide us with useful information about the effect of cooling rate on microstructure. It is observed that upon cooling (at cooling rate 4.2×10^{13} K s^{-1}), the number of both 1311 and 1321 bonded pairs reduces, indicating the fast cooling does not favour this kind of bonded pair.

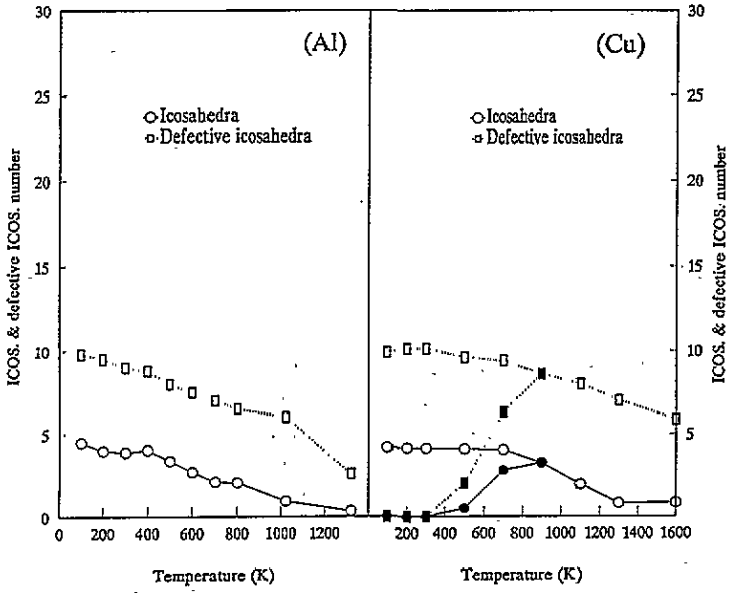

Figure 9. The relationship between the number of icosahedra and defective icosahedra and temperature during rapid solidification whose cooling conditions are the same as in figure 4.

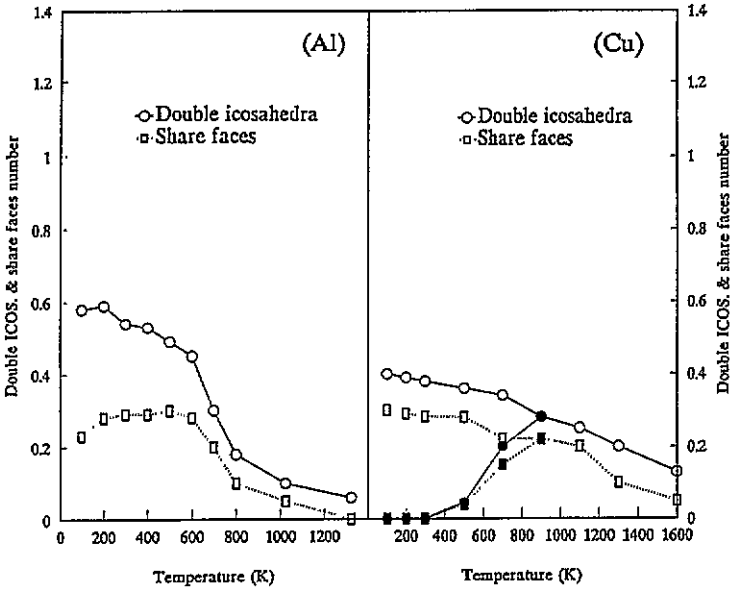

Figure 10. The relationship between the number of double icosahedra and common faces shared by different icosahedra and temperature during rapid solidification whose cooling conditions are the same as in figure 4.

Figure 9 represents the number of icosahedra and defective icosahedra for Al and Cu formed in liquid, supercooled and solid states during fast-cooling processing. It shows that on fast cooling, the number of both icosahedra and defective icosahedra increases, and the number of defective icosahedra is more than that of icosahedra. This may be the structure feature of the present metals. This result is consistent with the case of binary liquid alloys in our previous paper [40] at this point. It means that icosahedra are usually few in liquid, supercooled liquid and glasses compared with other kinds of defective icosahedron. In addition, it is further observed that icosahedra follow similar trends versus temperature as 1551 bonded pairs, $\overline{\text{ICOS}}Q_6$ and $\overline{\text{ICOS}}W_6$ do in pure metals (as in the case of binary liquid alloys, the 1551 bonded pairs follow the alternative rule compared with $\overline{\text{ICOS}}W_6$ as pointed out in our other paper [41], that is to say, the number of 1551 bonded pairs is a direct measurement of the number of icosahedra, whereas $\overline{\text{ICOS}}W_6$ is the measurement of the perfection of an icosahedron). Figure 10 illustrates the double icosahedra and common faces shared by different icosahedra counted in Al and Cu. Figure 10 demonstrates that in the whole temperature region studied here, the total number of double icosahedra is sparse even compared with icosahedra. It suggests that the icosahedra formed in pure Al and Cu are mostly single icosahedra. This result differs from binary liquid alloys [41] at this point. In the latter case, most of the icosahedra may be double icosahedra. Thus, that icosahedra formed in pure metals are mainly single icosahedra may be another feature of structure in the present simulation. Figure 11 presents the number of 1431 bonded pairs and Frank–Kasper polyhedra versus temperature. Figure 11 points out that the 1431 bonded pairs follow similar trends as 1541 bonded pairs; they are all the measurement on the short-range order in liquid and amorphous states [39]. The FK polyhedra in figure 11 seem very rare compared with other kinds of polyhedron, such as icosahedra and defective icosahedra, and

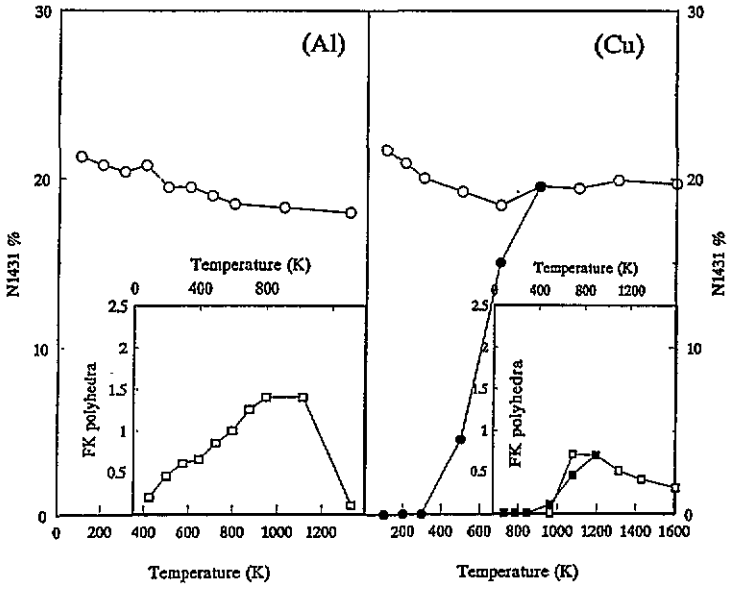

Figure 11. The relationship between the number of 1431 bonded pairs and FK polyhedra and temperature during rapid solidification whose cooling conditions are the same as in figure 4.

no Bernal hole polyhedra are detected in our study.

According to the definition of defective icosahedra, there exist several different ratios of 1441 to 1551 bonded pairs within defective icosahedra. They represent different types of defective icosahedron. Figure 12 presents these results. First, it tells us that these different types of defective icosahedron follow a similar trend to the defective icosahedra. Second, it shows that defective icosahedra with ratios of 1441 and 1551 bonded pairs equal to 1:10 and 2:8 take a relatively larger part, whereas defective icosahedra with ratios of 1441:1551 bonded pairs equal to 3:6 and 4:4 take smaller parts. This may be another structural feature of pure liquid metal Al and Cu.

5.2. Slow cooling and crystallization from liquid metals

In order to see if the EAM can be used to describe the crystallization behaviour from the liquid, we have adjusted the cooling rate at 800 K during the further cooling proceeding to 3.8×10^{11} K s^{-1} (relatively slower cooling rate in the present study). Figure 1(*b*) has illustrated the PCF at the cooling rate 3.8×10^{11} K s^{-1} and at 200 K. It clearly shows that the liquid metal Cu has been crystallized into FCC structure. Therefore, the EAM used in the present study can indeed provide a realistic description of crystallization behaviour from liquid metals. The bond orientational order parameters and pair analysis techniques adopted here will give detailed results on structural features. The solid symbols throughout figures 3(*b*)–12(*b*) for Cu display the bond orientational order parameters, various bonded pairs and polyhedra versus temperature upon cooling but at a relatively slower cooling rate 3.8×10^{11} K s^{-1} in the present paper. Figure 3(*b*) shows that the ICOSQ_6 and DEFQ_6 decrease when the cooling rate has been adjusted to 3.8×10^{11} K s^{-1}, and finally disappear, indicating no icosahedral symmetry exists. The TOLQ_6 seems to behave differently compared with

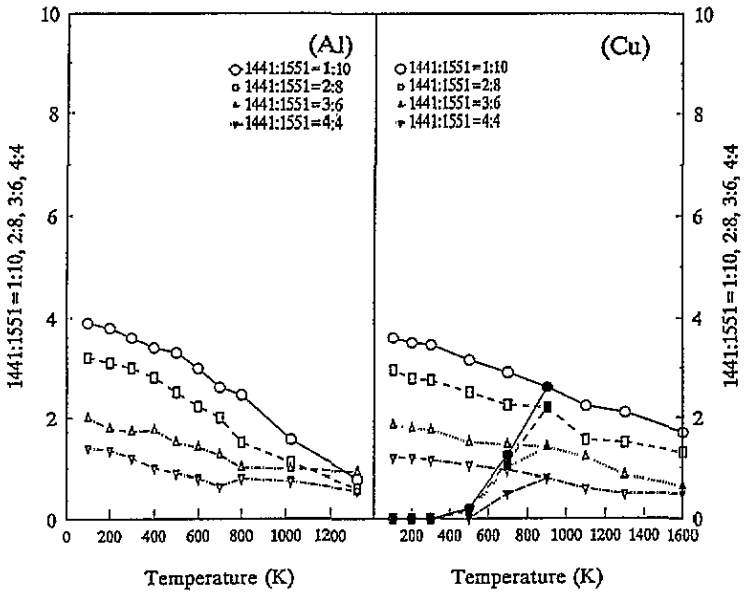

Figure 12. Defective icosahedra for Al (*a*) and Cu (*b*) with different ratios of 1441 to 1551 bonded pairs as labelled in the figure during rapid solidification, whose cooling conditions are the same as in figure 4.

ICOSQ_6 and DEFQ_6, and does not vanish in the further cooling processing. Therefore we cannot derive from TOLQ_6 any true information about crystallization; this may be due to the definition of calculation of TOLQ_6. Figure 4(*b*) shows the third-rotational invariant, W_6, of bond orientational order parameters upon the relatively slow cooling. It is observed that ICOSW_6 and DEFW_6 follow the same physical trend versus temperature as ICOSQ_6 and DEFQ_6. TOLW_6 behaves, however, as a different characterization feature compared with the quadratic-rotational invariant Q_6 of bond orientational order. At the relatively slow cooling rate 3.8×10^{11} K s^{-1}, the absolute value of TOLW_6 reduces, and at the final temperature of 100 K, it almost vanishes, indicating no icosahedra exist at all. Thus the third-rotational invariant TOLW_6 may be more sensitive to local symmetries than TOLQ_6, and thus may provide useful information about structural features. Figure 5(*b*) illustrates the number of 1551 and 1541 bonded pairs versus temperature at the slower cooling rate. It demonstrates that during the slow-cooling processing, both bonded pairs rapidly decreases and at 100 K, no fivefold symmetry of 1551 bonded pairs exists at all.

Figure 6(*b*) shows the characterization of the 1421 and 1422 bonded pairs. We derived from this behaviour that for slower-cooling processing the number of 1422 bonded pairs (HCP type) decreases, whereas that of 1421 bonded pairs (FCC type) increases, which is contrary to the situation of the fast cooling. Finally, at 300 K, apart from 1421 bonded pairs, no other kinds of bonded pair exist at all. It clearly demonstrates that the system has completely stepped to pure stable FCC structure, which is consistent with the PCF at 200 K in figure 1(*b*). Figure 7(*b*) shows the BCC-type symmetrical bonded pairs 1441 and 1661. It is shown that during the crystallization processing, both of these two bonded pairs decrease and eventually disappear at the final temperature. The solid symbols in figure 8(*b*) show the number of 1311 and 1321 bonded pairs during the crystallization processing. It is observed

that neither the relatively slow cooling rate nor the fast cooling favours the 1321 and 1311 bonded pairs. That is to say upon cooling processing, the threefold symmetry bonded pairs are gradually discarded in the present metal. Solid symbols in figures 9(*b*)–12(*b*) show icosahedra, defective icosahedra, double icosahedra, common faces and 1431 bonded pairs etc versus temperature during crystallization. We find that these physical quantities follow similar trends as the 1551, 1541 bonded pairs and, at the final temperature of 100 K, they all vanish.

6. Main conclusions

The results presented here have shown that the EAM functions parametrized to bulk solid properties can correctly and efficiently predict the glass transition and crystallization of liquid metals during rapid solidification. The calculated pair correlation functions are found to be in good agreement with experiments, especially for Cu.

During fast cooling at 4.2×10^{13} K s^{-1} in the present paper, the 1551, 1541 and 1422 bonded pairs increase, and the icosahedral ordering is gradually enhanced, whereas the 1441, 1661, 1321 and 1311 bonded pairs decrease to some extent, and 1421 bonded pairs vary slowly. In addition, it is found that during fast-cooling processing, the numbers of icosahedra, defective icosahedra and double icosahedra increase, and follow the same rule as the 1551 bonded pairs.

During crystallization of liquid Cu metal, the liquid metal finally transforms into a stable FCC structure which can be identified from the behaviour of the PCF. During this processing, the ICOSQ_6 sharply decreases and eventually disappears, indicating that no icosahedral ordering exists. Other kinds of bond orientational order and bonded pairs (except for TOLQ_6) have similar physical characteristics.

Acknowledgments

We would like to thank Professor Wang, at Waterloo University of Canada, for providing MD computer codes concerning cooling processing. Financial support provided by the Natural Science Foundation of China is gratefully acknowledged.

References

[1] Daw M S and Baskes M I 1983 *Phys. Rev. Lett.* **50** 1285
[2] Daw M S and Baskes M I 1984 *Phys. Rev.* B **29** 6443
[3] Johnson R A 1988 *Phys. Rev.* B **37** 3924
[4] Johnson R A 1988 *Phys. Rev.* B **37** 6121
[5] Johnson R A 1989 *Phys. Rev.* B **39** 12554
[6] Johnson R A 1990 *Phys. Rev.* B **41** 717
[7] Finnis M W and Sinclair J E 1984 *Phil. Mag.* A **50** 45
[8] Ackland G J and Thetford R 1987 *Phil. Mag.* A **56** 15
[9] Ackland G J, Tichy G, Vitek V and Finnis M W 1987 *Phil. Mag.* A **56** 15
[10] Ackland G J and Vitek V 1990 *Phys. Rev.* **1349** 2681
[11] Rosato V, Guillope M and Legrand B 1989 *Phil. Mag.* A **59** 321
[12] Norskov J K and Lang N D 1980 *Phys. Rev.* B **21** 2131
[13] Stott M J and Zaremba E 1980 *Phys. Rev.* B **22** 1564
[14] Foiles S M, Baskes M I and Daw M S 1986 *Phys. Rev.* B **33** 7983

[15] Daw M S, Baskes M I, Bisson C L and Wolfer W G 1986 *Modeling Environmental Effects on Crack Growth Processes* ed R H Jones and W W Gerberich (New York: Metallurgical Society of AIME)
[16] Daw M S 1986 *Surf. Sci. Lett.* **166** L161
[17] Foiles S M 1985 *Phys. Rev.* B **32** 3409
[18] Mei J and Davenport J W 1990 *Phys. Rev.* B **42** 9682
[19] Mei J, Davenport J W and Fernando G W 1991 *Phys. Rev.* B **43** 4653
[20] Mei J and Davenport J W 1992 *Phys. Rev.* B **46** 21
[21] Holender J M 1990 *J. Phys.: Condens. Matter* **2** 1291
[22] Holender J M 1990 *Phys. Rev.* B **41** 8054
[23] Kulp D T, Egami T, Luzzi D E and Vitek V 1992 *J. Alloys Compounds*
[24] Kulp D T, Ackland G J, Sob M, Vitek V and Egami T 1993 *Modelling Simul. Mater. Sci. Eng.* **1** 315
[25] Massobrio C, Pontikis V and Martin G 1989 *Phys. Rev. Lett.* **62** 1142
[26] Massobrio C, Pontikis V and Martin G 1990 *Phys. Rev.* B **41** 10486
[27] Holzman L M, Adams J B, Foiles S M and Hitchou W N G 1991 *J. Mater. Res.* **6** 298
[28] Rose J H, Smith J R, Guiner F and Fernate J 1984 *Phys. Rev.* B **29** 2963
[29] Sangster M J L and Dixon M 1976 *Adv. Phys.* **25** 247
[30] Frank F C 1952 *Proc. R. Soc.* A **215** 43
[31] Nelson D R and Toner J 1981 *Phys. Rev.* B **24** 363
[32] Steinhardt P J, Nelson D R and Ronchotti M 1981 *Phys. Rev. Lett.* **47** 1275
[33] Steinhardt P J, Nelson D R and Ronchotti M 1983 *Phys. Rev.* B **28** 784
[34] Honeycutt J D and Andersen H C 1987 *J. Phys. Chem.* **91** 4950
[35] Qi D W and Wang S 1991 *Phys. Rev.* B **44** 884
[36] Abraham F F 1980 *J. Chem. Phys.* **72** 359
[37] Liu R S, Qi D W and Wang S 1992 *Phys. Rev.* B **45** 451
[38] Aihara T Jr, Aoki K and Masumoto T 1994 *Mater. Sci. Eng.* A **199/180** 256
[39] Liu C F and Wang S 1992 *J. Phys.: Condens. Matter* **4** 6729
[40] Chen K Y, Liu H B and Hu Z Q *J. Phys.: Condens. Matter* at press
[41] Chen K Y, Liu H B and Hu Z Q *J. Chem. Phys.* at press
[42] Waseda Y 1980 *The Structure of Non-Crystalline Materials, Liquid and Amorphous* (New York: McGraw-Hill)